Hindawi
Geofluids
Volume 2022, Article ID 6558883, 19 pages
https://doi.org/10.1155/2022/6558883

Research Article

The Impact of Lamina Characteristics and Types on Organic Matter Enrichment of Chang 7_3 Submember in Ordos Basin, NW China

Congsheng Bian,[1] **Wenzhi Zhao**,[1] **Tao Yang**,[1] **Wei Liu**,[1] **Chaocheng Dai**,[2] **Xu Zeng**,[1] **Kun Wang**,[1] **Yongxin Li**,[1] **and Di Xiao**[2]

[1]*PetroChina Research Institute of Petroleum Exploration and Development, Beijing 100083, China*
[2]*East China University of Technology, College of Earth Sciences, Nanchang 330013, China*

Correspondence should be addressed to Congsheng Bian; biancongsheng@126.com

Received 4 February 2022; Accepted 17 May 2022; Published 18 June 2022

Academic Editor: Kouqi Liu

The Chang 7 member in Ordos Basin is an important shale oil exploration layer, with new shale-oil discoveries in recent years. The Chang 7_3 submember is rich in organic shale, which is the main source rock of shale oil in the Yanchang Formation. In order to clarify the lamina structure, composition, types, and distribution characteristics in Chang 7_3 submember and its influence on organic matter enrichment, a full coring well in Chang 7_3 submember located in deep-lacustrine facies is selected to obtain intensive systematic core samples. Core observation, thin section identification, X-ray fluorescence element analysis, X-diffraction analysis, scanning electron microscope, electron probe, rock pyrolysis, and other techniques are performed to systematically analyze the morphology, structure, thickness, mineral compositions, and organic matter content of the shale lamina in the Chang 7_3 submember. Five types of lamina are identified: silty felsic lamina (SF), tuffaceous lamina (TF), organic-rich clay lamina (ORC), organic-bearing clay lamina (OBC), and homogeneous clay lamina (HC), which are further subdivided into eight subtypes. The lamina types change greatly vertically in the Chang 7_3 submember, in which the lower part is mainly silty felsic lamina, organic-rich clay, and tuffaceous lamina, the middle part is mainly organic rich and organic clay lamina and organic-bearing clay lamina, and the upper part is mainly homogeneous clay lamina and a small amount of silty felsic organic-bearing clay lamina and organic-bearing clay lamina. Different laminae show various organic matter types, organic matter content (TOC), and organic matter occurrence states which can be divided into four occurrence types. The TOC in organic-rich clay lamina and part of homogeneous clay lamina is high, while that of silty felsic lamina is lower. The relationship between shale lamina and organic matter enrichment is established according to the correlation analysis of laminar characteristics, mineral content, and organic matter content. Among them, the organic-rich lamina is richest of TOC and is a favorable "sweet point" for shale oil exploration.

1. Introduction

Research on organic-rich shale has increasingly become a hotspot with the development of shale oil exploration in many basins. The lamina characteristics of fine-grained shale not only reflect the microstructure and quality of shale reservoir but also directly affect the fracture expansion law and fracturing effect of horizontal well volume fracturing [1–5]. Lamina study is an important content in fine-grained sedimentation, which contains lamina morphology, continuity, mineral composition, granularity change, and interface contact relationship [5–9], especially the formation mechanism of lamina [5, 10–15].

The classification of laminae is usually based on the organic matter as well as the composition and content of minerals. For example, Shi et al. [8] found that the Silurian Longmaxi Formation in Sichuan Basin developed four types of laminae, containing organic-rich, organic-bearing, clay, and silty; Xi et al. [9] thought that the shale of Chang 7_3

submember of Yanchang Formation in Ordos Basin includes four types of lamina: tuffaceous, organic, silty, and clay rich. As the most important and widely developed sedimentary feature in shale rock, lamina structure not only controls the reservoir physical properties of shale [16–21] but also leads to strong heterogeneity of shale reservoir, thus affecting the quality of shale reservoir. In particular, the lamina characteristics and types of continental shale are more complex than those of marine shale. Therefore, the study of laminar types and structures has become an indispensable content in the study of sedimentology in unconventional oil and gas, which has attracted the attention of geologists and explorers recently [22–24]. For example, Hua et al. [16] believe that the reservoir properties of coarse laminar shale of Longmaxi Formation in Sichuan Basin are better than thin laminar shale, and thin laminar shale is better than massive mudstone.

The types and characteristics of laminae are closely related to the lithology and lithofacies of shale. Exploration and research show that the lithology types of shale mainly include clay rich, siltstone and carbonate, or their combination [25–27]. Compared with lithology, the lithofacies types of shale are more complex [28]. In early studies, the lithofacies types of shale are usually divided according to mineral composition and organic matter content (TOC). The mineral composition usually includes felsic, clay, and carbonate, and TOC can be high or lower. For example, Wang and Carr divided the Marcellus Shale into seven types including organic siliceous shale, organic mixed shale, and gray mudstone [29]. Later, the sedimentary structure was considered in the lithofacies classification, which can generally be divided into laminated, beded, and massive. For example, Song et al. carefully made the lithofacies classification of Shahejie Formation shale in the Raoyang Sag according to the difference of rock type, sedimentary structure, and TOC [30]. Liu et al. divided the Qingshankou shale in the northern Songliao Basin into 7 lithofacies types according to the TOC, fabric, and mineral composition [31].

It is found that the shale of the Chang 7_3 submember in Ordos Basin has complex lithology, containing felsic, clay, sandstone, and siltstone, as well as the tuffaceous and carbonate, which results in diversified lamina structure and types, complex combination modes, and great differences in the distribution of mineral composition and organic matter in lamina [9, 22, 32]. The type, structure, and mineral composition of different laminae often control the type, enrichment, and occurrence characteristics of organic matter, thus affecting the hydrocarbon generation potential of organic matter and the quality of source rock [33]. In addition, the lamina influences the pore type and pore space distribution of shale, which in turn have an important impact on the content and occurrence of retained hydrocarbons [7, 34, 35].

Research also found that the organic-rich lamina shale in Chang 7_3 member of Ordos Basin is poor in porosity, but the situation in felsic rich shale is opposite, and the pore relatively developed [36, 37]. In addition, the TOC and porosity in tuffaceous and carbonate rich lamina are of great difference, which makes it more difficult to study formation mechanism of lamina, as well as the favorable area evaluation of shale oil exploration. Therefore, the fine research on the type, structure, and influence on organic matter enrichment of shale lamina in Chang 7_3 member is of great significance; however, the previous research in these aspects is relatively weak. Taking a fully cored well in Chang 7_3 member shale in the deep lacustrine faces as the research object, by systematic and intensive sampling, using thin section, X-ray diffraction analysis, scanning electron microscope, electron probe, and other analysis methods, combined with the principle of fine-grained sedimentology analysis, this paper describes the lamina types, structure, and mineral composition. Furthermore, the effects of laminar types on the occurrence forms and enrichment characteristics of organic matter are discussed in order to provide a reference for the enrichment characteristics and evaluation of shale oil in Chang 7_3 submember, Ordos Basin.

2. Geologic Background

Ordos Basin is a large superimposed basin in Central China, which is composed of six structural units, containing Western thrust belt, Tianhuan depression, Weibei uplift, Yimeng uplift, Yishan slope, and Jinxi fault-fold belt [38] (Figure 1(c)). During the sedimentary period of Yanchang Formation in the Late Triassic, the basin developed a large inland depression lake, deposited a set of clastic rock including lake and fluvial facies, which can be divided into 10 members from top to bottom (Figures 1(a)). The Chang 7 member in Yanchang Formation developed a greatest lake, and only the area of deep lacustrine faces can reach $6.5 \times 10^4\,km^2$, with abundant aquatic organisms and plankton, enrichment of organic matter, and black mudstone and shale [39]. The average thickness of Chang 7 member is about 80-100 m, of which Chang 7_3 submember is a section with concentrated distribution of organic-rich shale, with a cumulative thickness of 30-50 m (Figure 1(b)), rich in raspberry pyrite and Collophanite [40–42].

Ordos Basin is an important shale oil exploration field in China. The discovery of Qingcheng shale oil field in 2019 with 1 billion ton geological reserves has achieved a historic breakthrough in shale oil exploration progress in Chang 7 member. Moreover, Cy 1 and Cy 2 wells have obtained more than 100-ton oil flow per day in Chang 7_3 submember, with thick organic-rich shale and thin siltstone. In 2020, the shale oil output of Changqing Oilfield reached 143×10^4 t, realizing the scale benefit development of shale oil in Ordos Basin [39].

The core samples in this study are from the well that located in Wuqi area in the middle of Ordos Basin. The Chang 7_3 submember is a deep lacustrine faces deposit with a thickness of 46 m. The lithology is mainly shale mixed with siltstone and tuff. It can be divided into three positive cycles from top to bottom, by which Chang 7_3 submember is divided into three sublayers. A total of 152 samples are taken in the whole Chang 7_3 cores, with an average of 3 samples per meter (Figure 2), which makes a good foundation for the fine description of shale lamina types and structural characteristics.

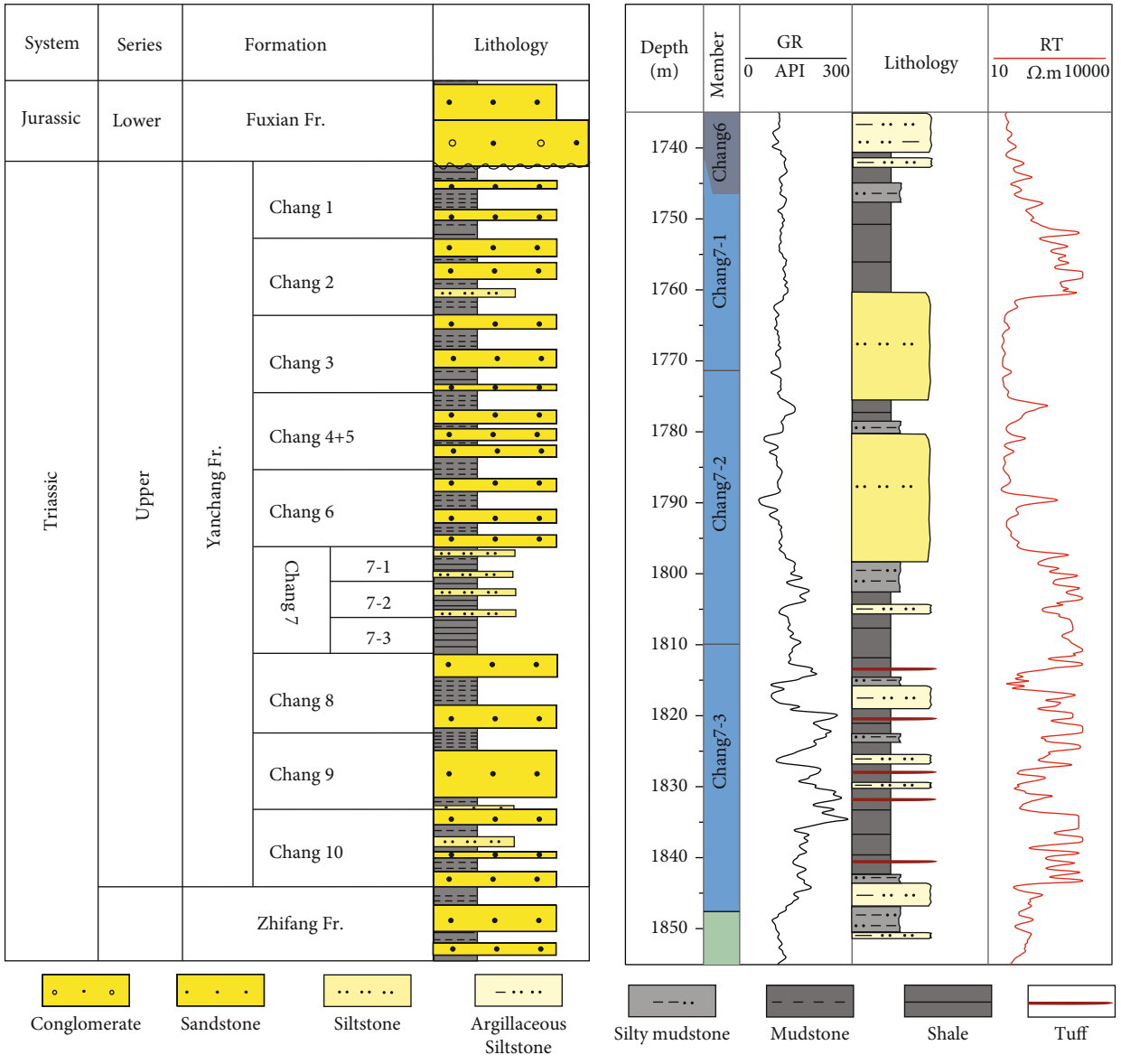

Figure 1: Continued.

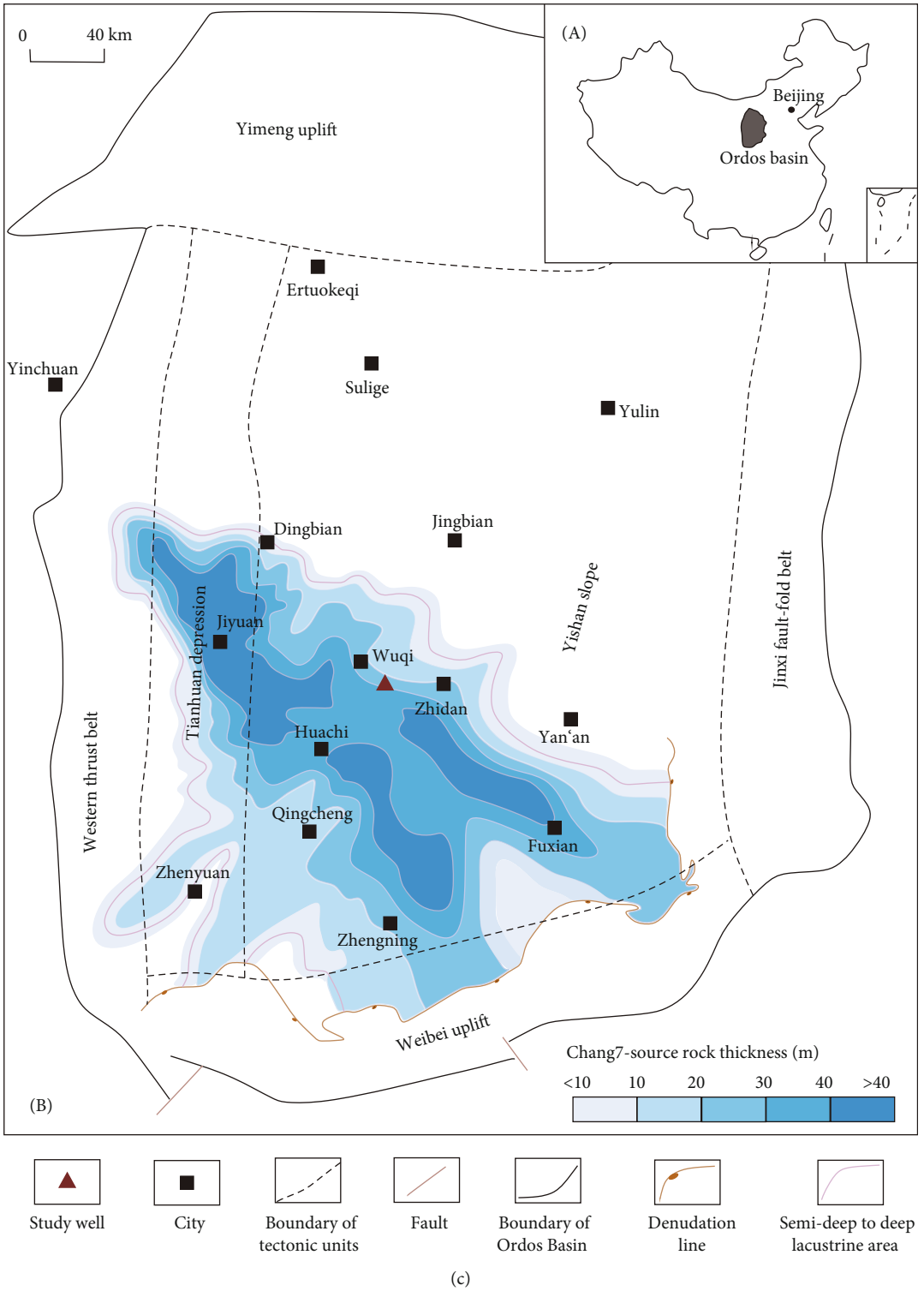

FIGURE 1: Comprehensive geological figure of Chang 7_3 member in Ordos Basin. (a) Stratigraphic histogram of Yanchang Formation (modified from [43]). (b) Well logging and stratigraphic histogram of Chang 7 member. (c) Sedimentary facies diagram of Chang 73 member (from [37]).

3. Data and Methods

Samples are from the cores of Chang 7_3 submember of Yanchang Formation in G well, with the depth of 1803.35~1853.5 m, and total 152 samples are analyzed with a sampling interval of 0.3-0.4 m. The lithology is mainly black shale, grayish black mudstone, dark gray silty shale, and brown tuff (Figure 2).

Shale lamina structures are analyzed by core description and thin section observation. The rock mineral composition

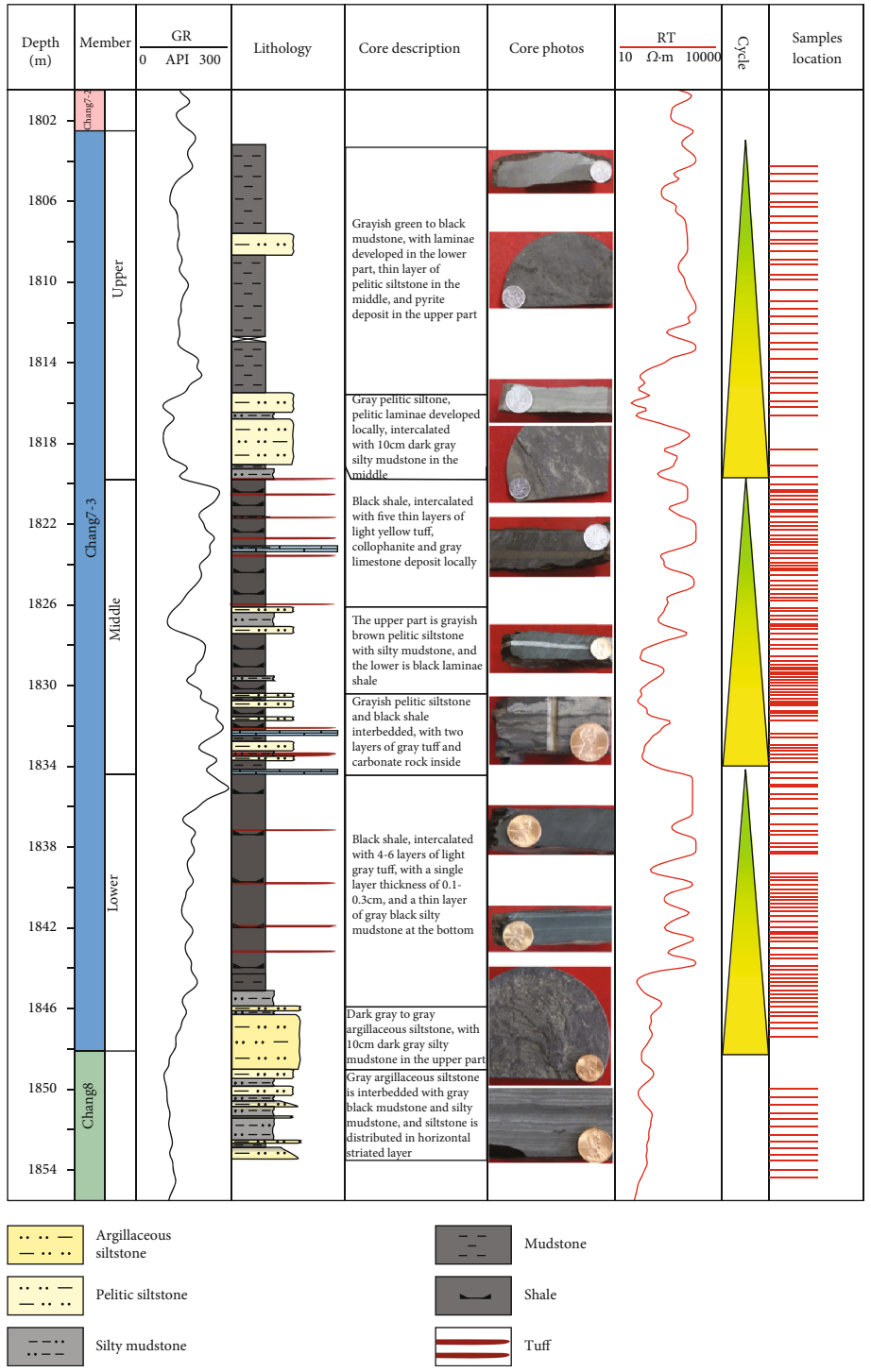

Figure 2: Core description and stratigraphic histogram of Chang 7_3 submember in Ordos Basin.

is determined by X-ray diffraction, scanning electron microscopy, and electron microprobe. Organic matter type and TOC value was obtained by CS-I carbon sulfur analyzer.

Optical microscope is the German Zeiss polarizing microscope, the eyepiece is 10 times, the objective lens is 5-20 times, single polarized light, and orthogonal transmission light. X-ray diffraction is done by d8advance X-ray diffractometer, which has Cu target, voltage 35 kV, and current 15 mA, and the analysis samples are 200 mesh powder. The scanning electron microscope is FEI Nova NanoSEM 450 thermal field emission scanning electron and Oxford Inca energy X-MAX 20 Oxford energy spectrometer. The test conditions are voltage 10 kV, current 86 Ma, and beam spot 3.5 μm, WD 5.0 mm. The electron probe adopts jeoljxa-

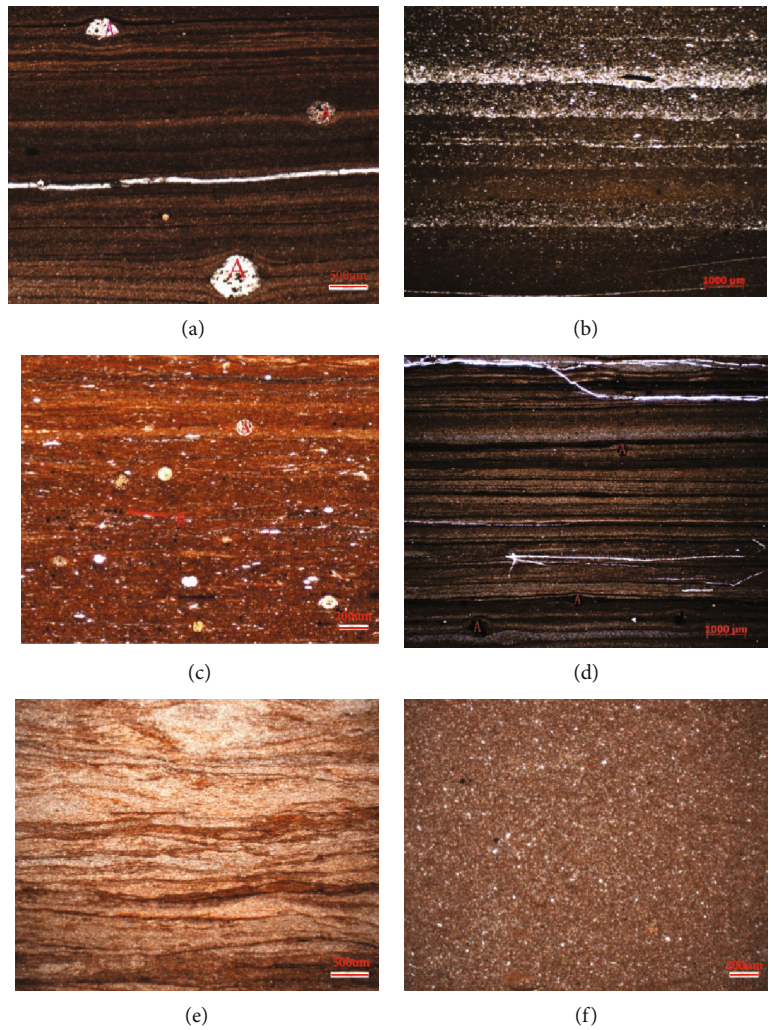

Figure 3: Micrograph of shale lamina of the Chang 7_3 member in Ordos Basin. (a) Extremely thin parallel plate-like lamina, algae (a) has strong anticompaction effect, 1830.00 m. (b) Thin parallel plate-like lamina, the content of quartz and feldspar in the lamina bottom is high, 1845.5 m. (c) Thin parallel plate laminae, high content of algae (a) and strawberry pyrite (b), 1832.9 m. (d) Extremely thin parallel plate-like laminae, black spots are strawberry pyrite (a), 1830.1 m. (e) Extremely thin parallel wavy lamina, 1827.1 m. (f) Homogeneous (block) bed, 1827.66 m.

Table 1: Average mineralogical composition for each section in Chang 7_3 member (unit: %).

Chang7_3 member	Quartz	Feldspar	Clay	Calcite	Dolomite	Pyrite	Others
Upper	21.3	15.3	57	1.9	0.3	3.1	1.1
Middle	17.9	21.3	42	2.5	7.5	6.4	2.4
Lower	21.1	23.2	47.7	1.9	2.6	1.6	1.9
Overall average	20.1	19.9	48.9	2.1	3.4	3.7	1.9

8800 m electron probe instrument. The working conditions are acceleration voltage 15 kV, probe current 10 mA, and beam spot diameter < 1 μm. The above three instruments accept the rock slices with Argon ion polishing and gold/carbon plating pretreatment. The CS-I carbon sulfur analyzer processes samples with 200 mesh powder and normal temperature and pressure.

4. Results

4.1. Lamina Structure. As for the lamina structure, different scholars have put forward different classification schemes according to the lamina thickness and shape [8, 44, 45]. Ingram called the lamina with thickness less than 3 mm as extremely thin lamina, the lamina with thickness of

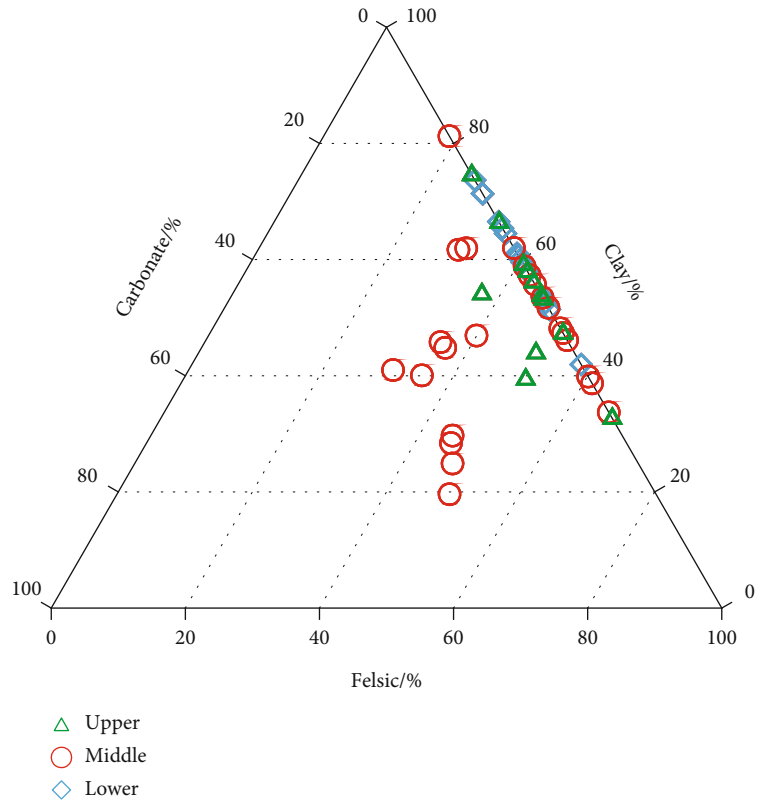

Figure 4: Ternary diagram of the bulk mineralogical composition of shale in Chang 7_3 member.

3 mm~1 cm as thin lamina, the lamina with thickness of 1 cm~3 cm as medium lamina, and the lamina with thickness of 3 cm~ 10 cm as thick lamina. From the perspective of lamina morphology, Campbell first divided lamina into three types: uniform lamina, wavy lamina, and curved lamina. For each type, it can be further divided into continuous parallel, intermittent parallel, continuous unparalleled, and intermittent unparalleled lamina [41]; Liu et al. put forward the concept of bright lamina and dark lamina shale of the Yanchang Formation in Ordos Basin, pointing out that the bright lamina is mainly made up of quartz and plagioclase, while the dark lamina mainly contains quartz and illite [42]. In the process of shale classification of Chang 7_3 member, predecessors mainly considered the lamina thickness and mineral composition and paid less attention to the lamina morphology. In this paper, based on the development form, thickness, and mineral composition of lamina, the lamina is divided into plate-like, wavy, and block types. Thereafter, according to the change of lamina thickness, the lamina with thickness less than 0.5 mm is called extremely thin lamina; the lamina with thickness of 0.5 mm~1 mm is thin lamina; the lamina with thickness of 1 mm~5 mm is medium lamina; the lamina with thickness of 5 mm~10 mm is thick lamina; this thicker than 10 mm is called bed.

The shale lamina in Chang 7_3 member of G well is mainly made up of extremely thin-thin plate-like laminae (Figures 3(a)–3(d)), and wavy as well as massive laminae is locally developed (Figures 3(e) and 3(f)). The plate-like laminae occur in continuous horizontal layers (Figures 3(a)–3(d)), in which the bright lamina and the dark one appear alternately. The bright lamina mostly contains quartz and feldspar, and the quartz particles are relatively bigger than other. The content of illite, mica, and other clay minerals as well as organic matter is higher in the dark lamina. The thickness of single lamina is mainly 0.05~1.0 mm (Figure 3(b)). The wavy laminae present near parallel wavy shape, and the bright lamina and dark one appear alternately too. Compared with the plate-like lamina, the clastic particles of the wavy lamina are finer, the single lamina is thinner, and the thickness is mainly distributed in 0.01~0.5 mm. The mineral composition in the bright and dark layer is similar to that in the plate-like lamina (Figure 3(e)). The massive lamina is dark brown to gray, with good homogeneity (Figure 3(f)), which is mainly composed of clay minerals and small amount of very fine silt. The clastic particles such as quartz and feldspar are rounded often, and clay minerals are mainly illite, with a maximum content of 80%, followed by quartz and feldspar, as well as a small amount of pyrite and muscovite, and the content of organic matter changes greatly.

4.2. Laminar Mineral Composition. The shale minerals in Chang7_3 member of Ordos Basin are mainly clay minerals, feldspar, quartz, calcite, and dolomite [43]. The X-ray diffraction test results of 152 samples from G well show that the mineral composition of Chang 7_3 shale is mainly clay and felsic (Table 1), and the clay mineral is mainly illite, containing a small amount of montmorillonite and kaolinite (Figures 4 and 5). The clastic minerals are mainly feldspar

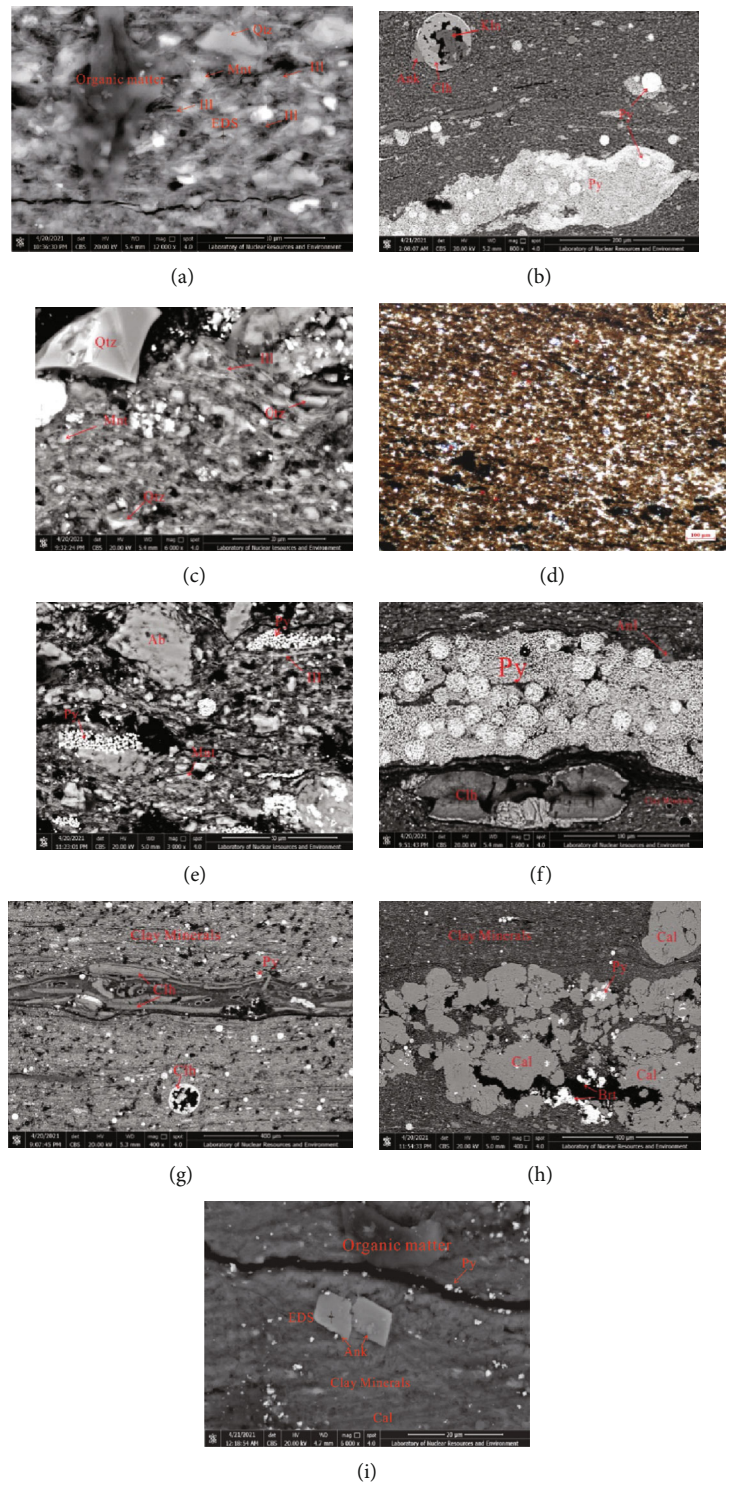

(a) (b) (c) (d) (e) (f) (g) (h) (i)

Figure 5: Micrograph of shale minerals of shale in Chang 7_3 member. (a) Illite (Ill) in clay minerals is in the shape of cotton wadding, hair, or long thin plate, 1830.00 m. (b) Authigenic kaolinite (Kln) shows the shape of authigenic sheet, which distributes in the inner cavity of algal fossils, 1845.5 m. (c) The surface of quartz particles (Qtz) is relatively smooth and produced in granular, lenticular, or strip shape, 1823.9 m. (d) Siliceous spots and veins, 1845.3 m. (e) Pyrite (Py) aggregates are produced in plate and strawberry shapes, 1825.25 m. (f) Pyrite (Py) aggregates of strawberry shapes, 1832.9 m. (g) Layered collophanite (Clh), 1832.9 m. (h) Spotted calcite (Cal), 1825.25 m. (i) Ankerite (Ank) single crystal is produced in self-shaped rhombic shape, 1821.85 m.

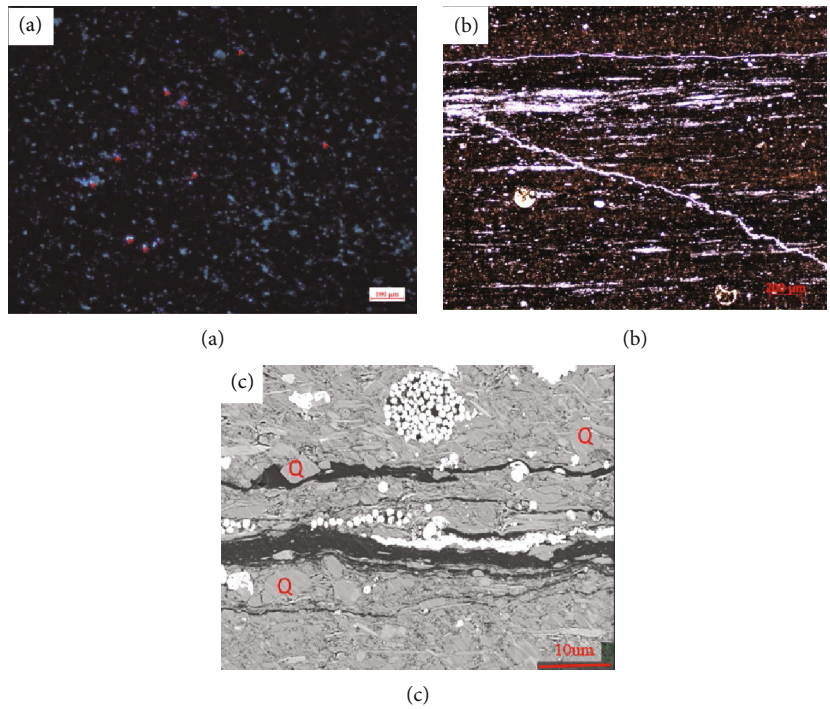

Figure 6: Micrograph of authigenic siliceous minerals in Chang 7_3 member. (a) Siliceous spots (red arrow) under fluorescent, 1845.3 m. Single polarized photo is shown in Figure 5(a); (b) siliceous veins, 1841.8 m; (c) SEM photos of siliceous spots, Q in the figure is authigenic quartz, 1841.8 m.

and quartz, with an average content of 40%. Only in the middle part of the Chang 7_3 submembers, there are 20-30% proportion of calcite and dolomite (Figure 4). The content of clay minerals varies greatly, mainly 42-57%, with an average content of 48.9%. According to the observation of scanning electron microscope, illite in clay minerals is in the shape of cotton wadding, hair, or long thin plate (Figure 5(a)), symbiotic with fine quartz and montmorillonite. Montmorillonite is spherical or lenticular, weakly oriented under the influence of compaction (Figure 5(b)). Authigenic kaolinite shows the shape of authigenic sheet, which distributes in the inner cavity of algal fossils (Figure 5(b)), indicating the existence of late low-temperature hydrothermal process. The mineral compositions of algae are iron dolomite→pyrite (PY)→collophanite (CLH)→iron dolomite (ANK)→organic matter(O-M)→authigenic kaolinite (KLN) from outside to inside.

In the clastic minerals of Chang 7_3 shale, the content of quartz is about 15-40%, with an average of 20.1%. The surface of quartz particles is relatively smooth and produced in granular, lenticular, or strip shape (Figure 5(c)). Plagioclase content is about 5-32%, with an average of about 14.5%. Albite is produced in thin plate, granular and angular shape. Dissolution holes are developed in the particles and filled with organic matter. More special, siliceous spots and veins are relatively developed (Figures 5(d)), which commonly show fluorescence (Figure 6). In order to understand its genesis, the siliceous area was analyzed in detail by electron microprobe (Table 2). The data shows that the content of SiO_2 is basically more than 50%, and the content of aluminum, potassium, and sodium minerals is also high, indicating a good associated relationship with feldspar. It is considered that the spotted and vein quartz comes from the dissolution and precipitation of SiO_2 from feldspar. The formula is as follows [46]:

(1) $3KAlSi_3O_8(\text{potassium}) + 2H^+ + H_2O = KAl_3Si_3O_{10}(OH)_2(\text{illite}) + 6SiO_2(\text{siliceous}) + 2K^+ + H_2O$

(2) $3NaAlSi_3O_8(\text{albite}) + K^+ + 2H^+ + H_2O = KAl_3Si_3O_{10}(OH)_2(\text{illite}) + 3Na^+ + 6SiO_2(\text{siliceous}) + H_2O$

Oval authigenic quartz is symbiotic with rectangular irregular feldspar and clay, indicating that there is a genetic relationship between them, and there is no obvious crystal form of quartz (Figure 6(c)). This phenomenon is mainly found in the shale of middle and lower part of Chang 7_3 member.

Pyrite is mainly sulfide of Chang 7_3 member shale, with a diameter of 1.1-25 μm, self-shaped crystal of quadrilateral, hexagonal, or colloidal. The aggregates of pyrite are like strawberry, radial, lenticular, and other forms (Figures 5(e) and 5(f)). Pyrites in different aggregates have complex contact relationships and multistage growth characteristics. Collophanite is common in Chang 7_3 member shale, with a diameter of 10 μm-2.5 mm, in shape of plate, crescent, or ring. The aggregate of collophanite shows banded, lenticular, or irregular (Figure 5(g)). Collophanite is partially transformed into apatite and calcite during diagenesis.

The content of carbonate in Chang 7_3 member is relatively small, which is mainly composed of calcite, ankerite. Calcite often developed dissolution holes and later filled with

Table 2: EPMA data in siliceous area of Chang 7_3 member shale (unit: %).

Number	Depth	Na_2O	K_2O	SiO_2	FeO	CaO	Al_2O_3	P_2O_5	MgO	Total
1	1828.8	0.928	1.543	97.221	0.944	1.33	9.153	0.448	0.434	99.001
2	1849.9	0	0.003	96.886	0.193	0.011	0.019	0.036	0	97.148
3	1849.9	0	0.007	95.985	0.09	0.005	0	0.032	0.002	96.121
4	1849.9	0	0.016	94.323	0.201	0.002	0	0	0.02	94.562
5	1846.5	0.023	0.013	93.162	0	0.032	0.023	0	0.024	93.277
6	1846.5	0	0	91.867	0.073	0.025	0.021	0.032	0	92.018
7	1826.55	0	0.033	87.185	0.129	0.052	0.978	0	0	88.377
8	1805.15	0	0	81.133	0.039	0.035	0.007	0.036	0	81.25
9	1820.5	2.886	1.774	77.479	1.183	0.227	10.578	0.035	0.405	94.567
10	1808.25	7.076	0.452	76.272	0.189	7.204	1.305	0	3.972	96.47
11	1818.75	11.013	0.441	72.763	0.171	0.15	18.064	0.004	0.119	99.725
12	1818.75	7.167	2.081	69.812	0.409	0.775	16.259	0.106	0.331	96.94
13	1820.1	1.797	2.17	68.732	0.34	0.261	9.116	0.024	0.158	82.598
14	1808.25	6.533	0.448	66.423	0.342	6.682	1.432	0.039	3.385	85.284
15	1818.75	1.031	13.851	66.292	0.114	0.027	16.934	0.03	0	98.279
16	1850.6	2.967	5.735	65.565	0.521	0.383	16.868	0.004	0.175	92.218
17	1828.7	3.644	4.087	64.32	0.55	1.041	16.682	0.047	0.139	90.51
18	1805.15	1.502	14.146	64.312	0.111	0.057	17.243	0	0	97.371
19	1827.3	3.104	11.17	63.37	0.253	0.163	16.933	0.008	0	95.001
20	1828.7	4.531	2.164	62.531	0.714	1.01	14.229	0.047	0.214	85.44
21	1827.66	1.03	13.279	61.776	0.148	0.827	17.499	0.261	0	94.82
22	1850.6	1.071	16.88	61.373	0.218	0.041	15.126	0.013	0	94.722
23	1821.85	0.249	1.276	58.615	1.49	0.553	24.981	0.023	3.069	90.256
24	1828.7	1.918	2.675	57.923	2.091	2.149	11.823	0.719	0.648	79.946
25	1830	0.885	4.025	56.185	5.376	0.685	21.317	0.119	2.302	90.894
26	1843	7.663	0.148	55.233	0.05	10.764	24.159	0.004	0	98.021
27	1827.3	6.927	1.167	54.993	0.118	10.338	13.716	4.664	0.117	92.04
28	1819.15	1.807	3.408	54.641	1.878	0.679	18.715	0.108	1.407	82.643
29	1850.6	1.687	15.058	53.981	0.026	0.055	13.762	0.013	0	84.582
30	1833.7	1.063	3.441	53.776	3.096	1.645	12.782	1.109	1.242	78.154

pyrite and organic matter (Figure 5(h)). The ankerite crystal occurs with rhombic and bicrystals (Figure 5(i)).

4.3. Laminar Types. Based on the analysis of morphology, thickness, mineral composition, and TOC value, the lamina of Chang 7_3 member constitutes five types: silty felsic lamina (SF), tuffaceous lamina (TF), organic-rich clay lamina (ORC), organic-bearing clay lamina (OBC), and homogeneous clay layer (HC) (Table 3 and Figure 7), which are further subdivided into eight subcategories.

(1) *Silty Felsic Lamina (SF).* The grain in the lamina is mainly feldspar and quartz, with a content of up to 60-70%, but the content of organic matter is low, only 1-5%. This lamina shows light color, developing silt grade positive grain sequence, and particle size decreases upward as well as clay content increases, with the main particle size of 10-50 μm. The minerals are sorted medium to good, and the thickness of a single lamina is about 0.4 mm-10 mm (Figure 7(a)).

(2) *Tuffaceous Lamina (TF).* The lamina is mainly light gray volcanic tuff material, occurring nearly horizontal, including angular volcanic glass and crystal chips, interbedded with intermittent organic matter bands. Authigenic pyrite is widely developed where tuffaceous matter often contacts banded or dispersed organic matter. The content of organic matter is about 3-5%, and the thickness of a single lamina is about 0.2-1 mm.

(3) *Organic-Rich Clay Lamina (ORC).* The lamina can be further subdivided into two subtypes. ① Organic-rich plate-like clay lamina: this lamina has a dark color and presents a horizontal mud grade structure, in which a small amount of bright color striated lamina occurs, showing high content of felsic. The thickness of a single lamina is about 0.1-1 mm. A great amount of dispersed organic matter fragments, algal fossils, and collophanite can be seen, and the content of organic matter is about 8-12% (Figures 7(c) and 7(d)). ② Organic-rich wavy clay

Table 3: Shale lamina type division scheme of shale in Chang 7_3 member.

Code	Types	Subtypes	Key attributes
SF	Silty felsic lamina	/	Composition: silty quartz (30%~40%), feldspar (30%~40%), and clay minerals (20%~40%) Structure: coarse grain; structure: the single lamina is lenticular or linear, locally wavy, continuous, or intermittent, and the lamina is superimposed in parallel or nonparallel
TF	Tuffaceous lamina	/	Composition: clay minerals (5%~10%), other clastic minerals (70%~90%), and organic matter (3%~5%) Structure: fine grain; structure: the single lamina is continuous or intermittent plate-like in parallel
ORC	Organic-rich clay lamina	Organic-rich plate-like clay lamina Organic-rich wavy clay lamina	Composition: clay minerals (50%~75%), other clastic minerals (10%~20%), and organic matter (6%~15%) Structure: fine grain; structure: the single lamina is continuous plate-like or wavy in parallel
OBC	Organic-bearing clay lamina	Organic-bearing tabular clay lamina Organic-bearing wavy clay lamina	Composition: clay minerals (50%~75%), other clastic minerals (15%~25%), and organic matter (3%~6%) Structure: fine grain; structure: the single lamina is continuous plate-like or wavy in parallel
HC	Homogeneous clay layer	/	Composition: clay minerals (50%~75%), other clastic minerals (8%~20%), and organic matter (2% 10%) Structure: fine grain; structure: massive, with no obvious bedding

lamina: this lamina is yellow to brownish red and also presents mud grade structure. Clay minerals and organic matter form wavy lamina in lenticular and gentle waves. The thickness of a single lamina is about 0.05-0.5 mm. The organic matter content is about 6-12% (Figure 7(e)).

(4) *Organic-Bearing Clay Lamina (OBC)*. This lamina has a similar structure and mineral composition to organic-rich clay lamina. It is also further subdivided into two subtypes according to the lamina shapes: ① organic-bearing plate-like clay lamina, which is brownish yellow and a low content of organic matter about 3-6% and ② organic-bearing wavy clay lamina. Clay minerals and organic matter form wavy lamina in lenticular or gentle wavy shape. The thickness of a single lamina is about 0.05-0.5 mm. The organic matter content is about 4-5% (Figures 7(f) and 7(g)).

(5) *Homogeneous Clay Bed (HC)*. This lamina is further subdivided into two subclasses according to the content of organic matter. ① Homogeneous organic-rich clay bed: this lamina is black or gray black as to plenty of clay minerals and organic matter, showing a mud clastic structure, and light colored felsic particles dot it. The thickness of the single layer is greater than 10 mm, and the content of clay and organic matter is about 50-80% and 6-10%, respectively (Figure 7(h)). ② Homogeneous organic-bearing clay bed. The lamina has lighter color compared with the former, because of lower content of organic matter, only 2-6% (Figure 7(i)).

4.4. Longitudinal Distribution of Lamina. Through the statistical analysis of the core samples, extremely thin and thin plate-like lamina are mainly types in Chang 7_3 submember of well G, and wavy lamina or massive bed develop locally. Moreover, the organic-rich clay lamina most developed, mainly in the middle and lower part of Chang 7_3 member (Figure 8), and the TOC is basically more than 8%. The organic-bearing clay lamina is distributed almost whole Chang 7_3 member, which is complementary to the distribution of organic-rich lamina and homogeneous clay bed, and homogeneous clay bed developed mainly in the up part of Chang 7_3 member. The silty lamina mainly distributes at the top and bottom part where the siltstone deposits, and the tuffaceous lamina occurs mainly at the lower and the middle part. The proportion of these two laminas is relatively low, less than 20%. What conditions may affect this combination? What is the impact on organic matter enrichment?

Several combinations of laminar types often occur in the same depth section from Figure 8, which is related to the complex sedimentary environment [8] and the influence of external material events during the deposition of Chang 7_3 member in Ordos Basin. In the middle and lower part of Chang 7_3 member, the shale of semideep to deep lacustrine facies [47] is mainly deposited, which usually develops ORC and OBS lamina combination. However, at the same time, volcanic events [32] and gravity flow [48] occurs often, and the SF and TF laminae are developed. In the upper part, the shale and mudstone mainly deposit under the semideep lacustrine environment. Meantime, affected by gravity flow and terrigenous input, a small amount of SF and OBC lamina combination developed.

4.5. Characteristics and Types of Organic Matter in Lamina. The type of organic matter has a great influence on its hydrocarbon generation capacity and the types of generation products [49, 50]. The results of slices analysis show that the shale of Chang 7_3 submember is mainly sapropelic and

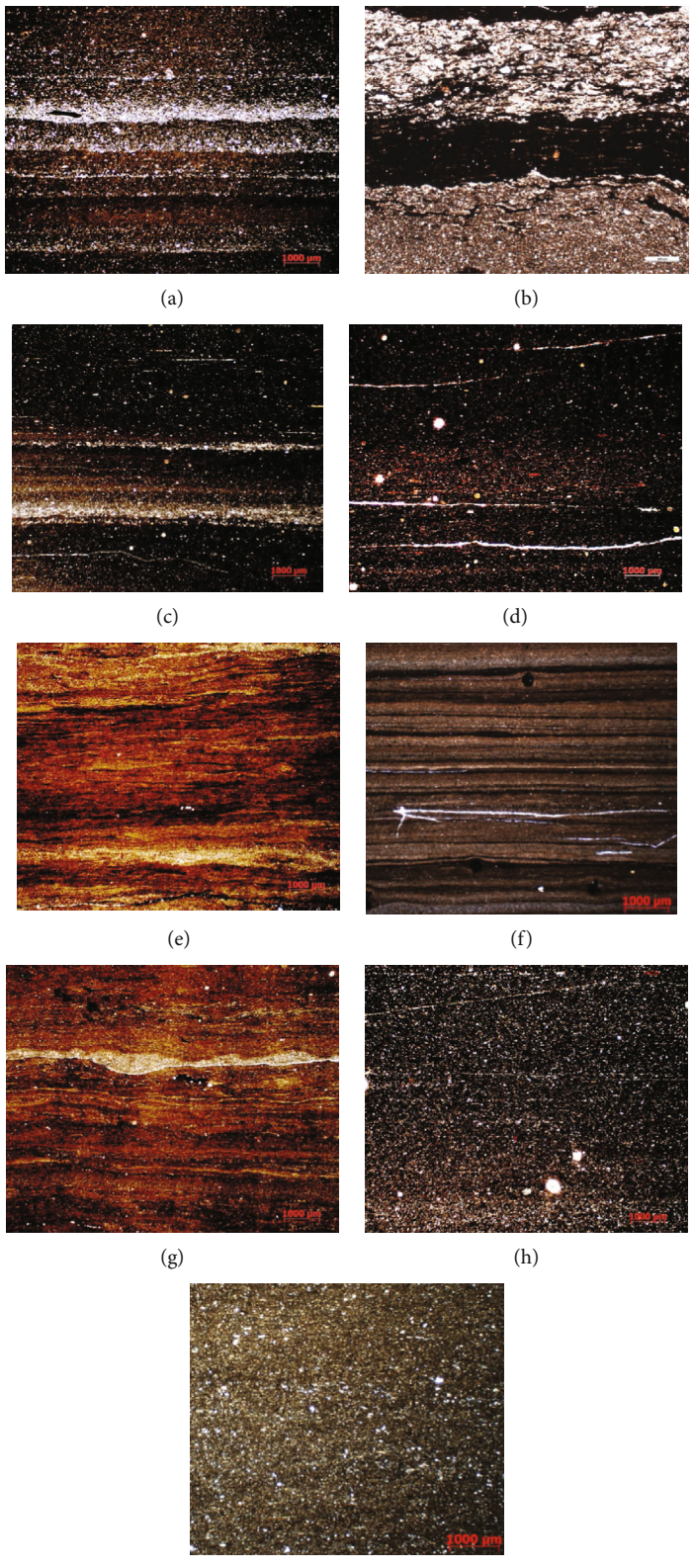

Figure 7: Micrograph of shale lamina types of the Chang 7_3 member in Ordos Basin. (a) Silty felsic lamina, 1845.5 m. (b) Tuffaceous lamina, 1833.4 m. (c) Organic-rich plate-like clay lamina, 1833.7 m. (d) Organic-rich plate-like clay lamina, 1824.5 m. (e) Organic-rich wavy clay lamina, 1826.8 m. (f) Organic-bearing plate-like clay lamina, 1825.5 m. (g) Organic-rich plate-like clay lamina, 1824.5 m. (h) Organic-bearing wavy clay lamina, 1825.4 m. (i) Homogeneous clay layer, 1844.8 m.

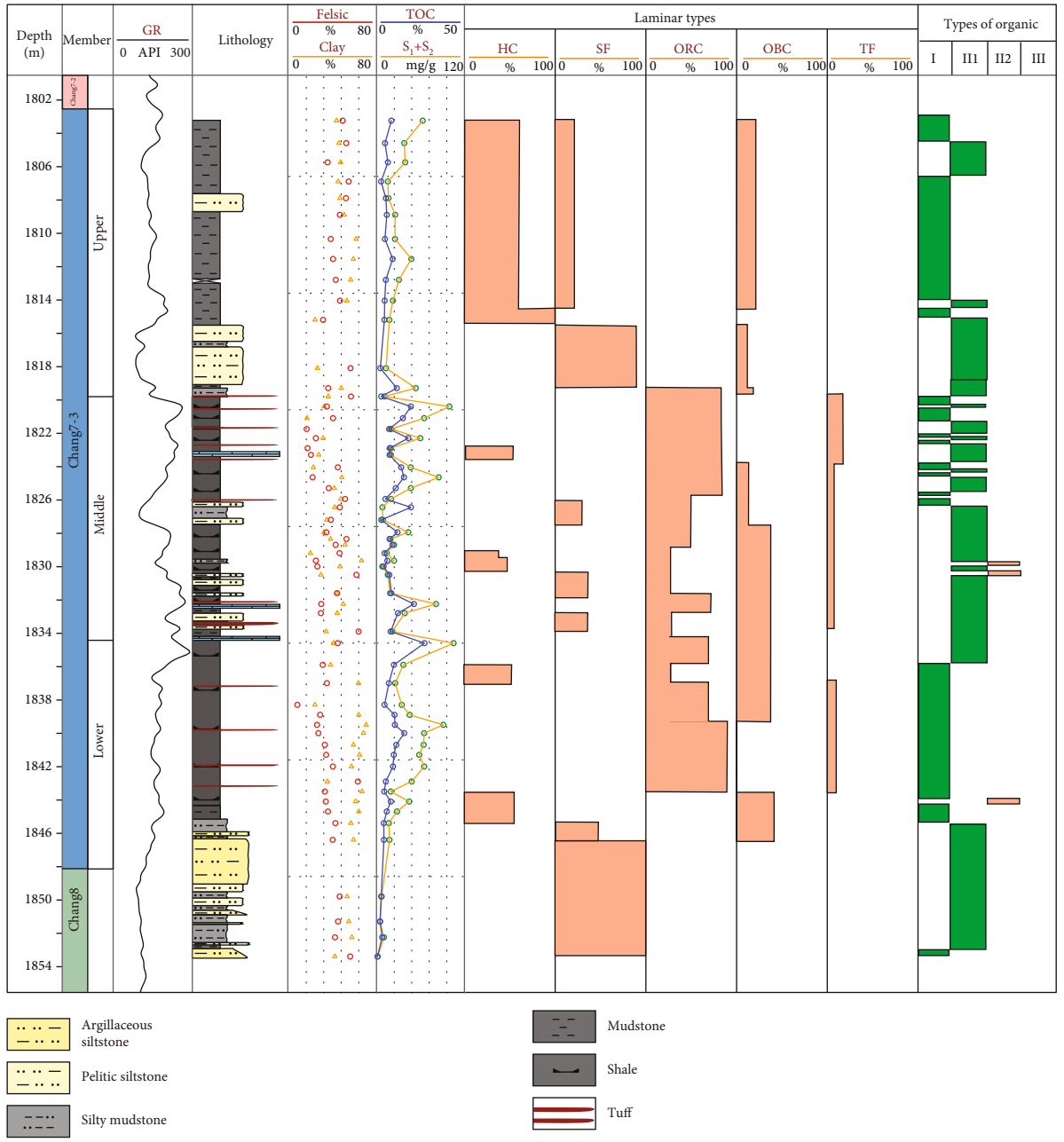

Figure 8: Shale lamina types and distribution of the Chang 7_3 member in Ordos Basin.

vitrinite, accounting for 68.8% and 22.7%, respectively, followed by crustite, inertinite, and secondary organic units. Sapropelic is mainly composed of structural algae, layered algae, and asphaltene, which all accounts for about 0.9% of the whole rock. Vitrinite is mainly composed of hydrogen rich vitrinite, normal vitrinite, and recycled vitrinite, accounting for about 1.2% of whole rock. It is flaky and structureless under microscope. Exinite is mainly composed of sporopollen, cutinite, corkite, resinite, and shell debris, only accounting for 0.2% of whole rock and 4.2% of the relative maceral content. Inertinite is mainly composed of filaments, coarse stereoliths, fungi, and inertinites, only accounting for about 0.1% of whole rock and 2.6% of the relative macerals. The secondary organic units are mainly composed of hydrogen-rich and hydrogen-poor secondary components, only accounting for 0.1% of whole rock and 1.7% of the relative macerals.

Shale in Chang 7_3 submember contains high sapropelic and vitrinite group and has high hydrogen index (between 300-700 mg/g.TOC). It can be clear from the cross plot of hydrogen index (IH) and Tmax that kerogen types are mainly type I and type II_1, with great hydrocarbon generation potential and oil generation (Figure 9).

4.6. Distribution Characteristics of Organic Matter in Lamina. Through the observation of microscope and scanning electron microscope, the organic matter in Chang 7_3 member shows four occurrence forms: ① dense

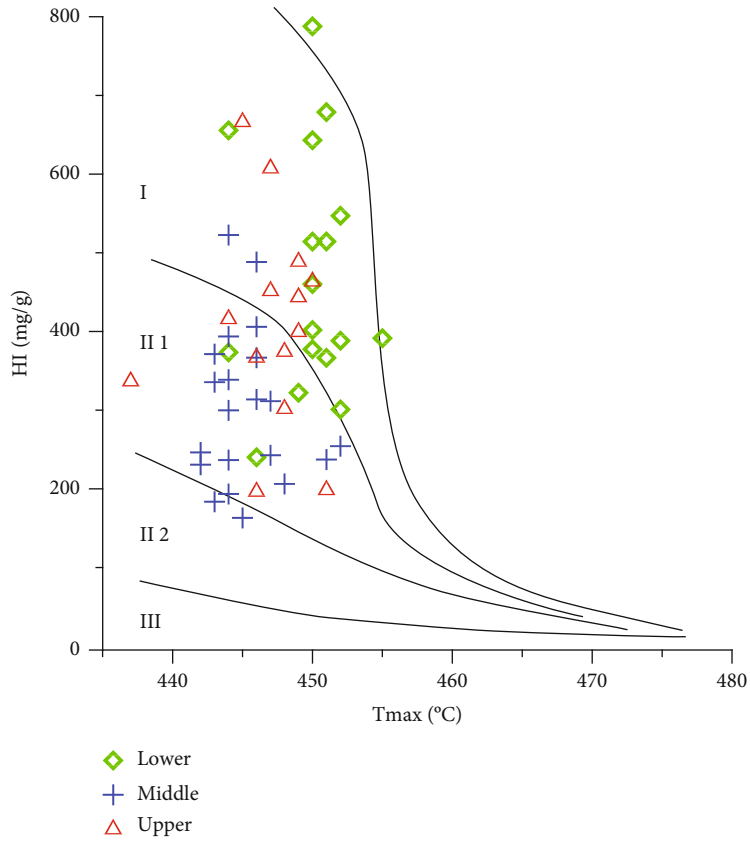

Figure 9: Classification of shale organic matter types of the Chang 7_3 member in Ordos Basin.

disseminated: the organic matter is densely disseminated and evenly distributed (Figures 10(a) and 10(b)), and the average TOC is about 10%. This type is mainly distributed in plate-like clay lamina and homogeneous clay bed, with low content of felsic, and the thickness of single lamina is usually large; ② sparsely dispersed: organic matter is dispersed in shale (Figures 10(c) and 10(d)), and the TOC is low, mostly less than 8%. This type mainly distributed in silty felsic lamina and clay layer. The content of felsic or clay is high, and the lamina is thin, usually 0.1-0.05 mm; ③ vein and lenticular like; organic matter is densely distributed in vein and lenticular shape (Figure 10(e)), which is often symbiotic with pyrite and collophanite. The TOC is usually high, mostly more than 8%. This type is mainly distributed in organic-rich clay lamina. According to the statistical data, the thinner the lamina, the higher the content of organic matter is. ④ Lamina-like; organic matter is distributed in relatively continuous lamina (Figure 10(f)), but the density of organic matter lamina is low, so the TOC is also low (3-8%), which is mainly distributed in thin parallel plate lamina.

5. Discussion

5.1. Effect of Lamina on Organic Matter Types and TOC. The analysis results of 152 shale samples show that the organic matter types of Chang 7_3 member shale are mainly type I and type II_1, and the organic matter types of different types of laminae are significantly different (Figures 8 and 9). The organic matter in organic-rich clay lamina, tuffaceous lamina, and homogeneous clay layer is mainly type I; however, the organic matter types of silty felsic lamina and organic-bearing clay lamina are mainly type II_1. Qiu et al. also put forward that the organic-rich shale of Lucaogou Formation in the Jimusar Sag contained mainly type I–II_1 kerogen, while the silty shale often deposited type II_1–II_2 kerogen [26]. This is related to the fact that different laminae represent different sedimentary environments and different hydrodynamic conditions. The deposit hydrodynamics of silty felsic lamina is relatively strong, the oxygen content of water body is high, and the organic matter is mainly from land input. The deposit hydrodynamic conditions of organic-rich clay lamina are between silty felsic lamina and homogeneous clay layer. Under relatively weak hydrodynamic conditions, aquatic algae dominated by plankton are easy to deposit, and the organic matter is dominated by lipid compounds (Figures 3(c) and 10(a)). Therefore, this kind of lamina has good organic matter type and high TOC. This is consistent with the understanding of the formation environment of lamina types of Longmaxi formation in Sichuan Basin discussed by Shi et al. [8].

However, there are two different kerogen types in the homogeneous clay layer, and the content of organic matter is quite different. Among them, the hydrodynamic conditions of the homogeneous clay layer rich in organic matter are the weakest, and the oxygen content at the bottom of

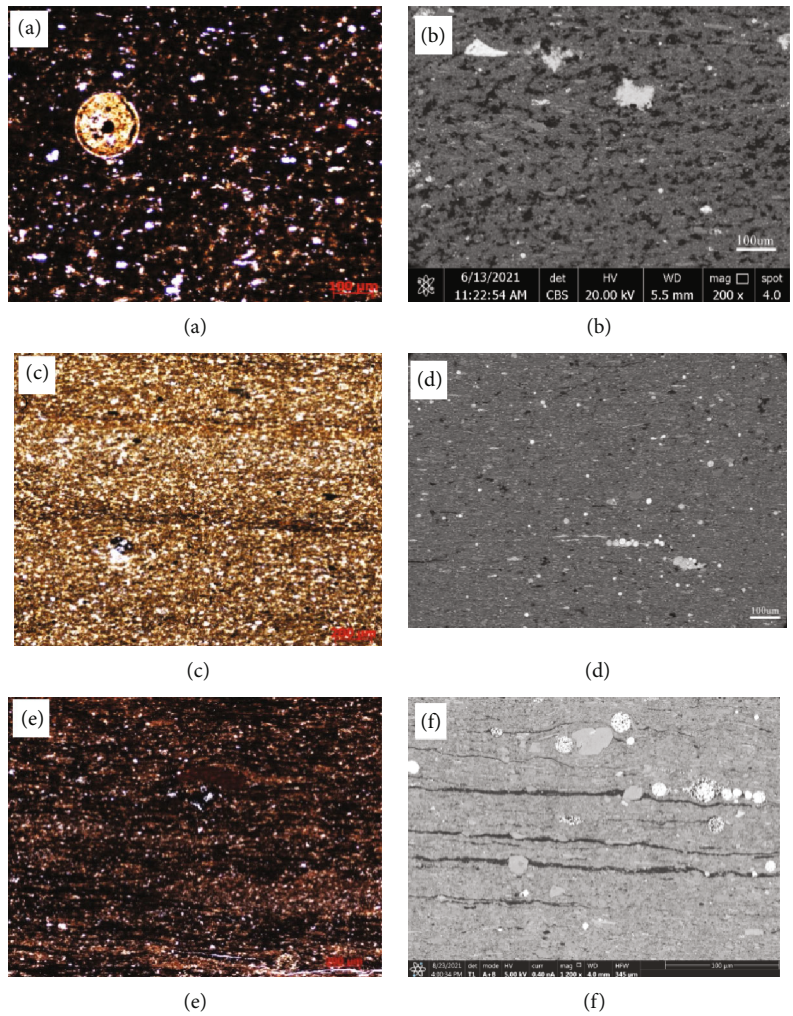

Figure 10: Microscopic characteristics of shale organic matter distribution of the Chang 7_3 member. (a) Dense disseminated organic matter, 1826.05 m. (b) Dense disseminated organic matter, 1828.7 m. (c) Sparsely dispersed organic matter, 1832.9 m. (d) Sparsely dispersed organic matter, 1821.85 m. (e) Vein and lenticular-like organic matter, 1830.6 m. (f) Lamina-like organic matter, 1814.15 m.

the water is lower, which is conducive to the preservation of organic matter. Therefore, the content of organic matter is mostly more than 6%, and the organic matter is densely disseminated. The content of felsic in the homogeneous clay layer containing organic matter is high, indicating that there are certain hydrodynamic conditions and relatively poor preservation conditions. The main organic matter is type II_1, and the abundance of organic matter is also low. The tuffaceous lamina itself does not contain organic matter, but volcanic ash can bring a lot of nutrients. Algae and collophanite are developed on both sides of the tuffaceous lamina (Figure 7(b)). Therefore, although the content of organic matter in tuffaceous lamina is relatively low, it can promote the growth of organic matter in other lamina. Zhang et al. [33] and Liu et al. [51] also proposed that volcanic eruptions form a large amount of nutrients, which has a "fertilization" effect on aquatic organisms in the lake.

5.2. Effect of Lamina Mineral on Organic Matter Enrichment. Through the statistical analysis of the relationship between mineral composition and organic matter enrichment of different types of laminae, the TOC of shale in Chang7_3 member is generally negatively correlated with quartz and feldspar and positively correlated with pyrite, but no obvious relationship with clay minerals (Figure 11). Previous studies [52] have shown that the higher the content of felsic, the increase of terrigenous substances, good water fluidity, and high oxygen content. It is not easy to preserve after biological death, which is not conducive to the enrichment of organic matter. The deposition of pyrite requires still water and strong reduction environment. Therefore, the increase of pyrite content indicates that the water body has strong reduction, which is conducive to the preservation of organic matter. For different types of laminae, the mineral content of silty felsic laminae changes the most with the TOC. For example, when the TOC increases from 0% to 5%, the content of feldspar and quartz decreases from 40% to 15-20% (Figure 11), while the content of clay increases from 30% to 60%, which indicates that the change of terrestrial input and water energy has the greatest impact on the change of TOC in this kind of lamina. Related to other types of

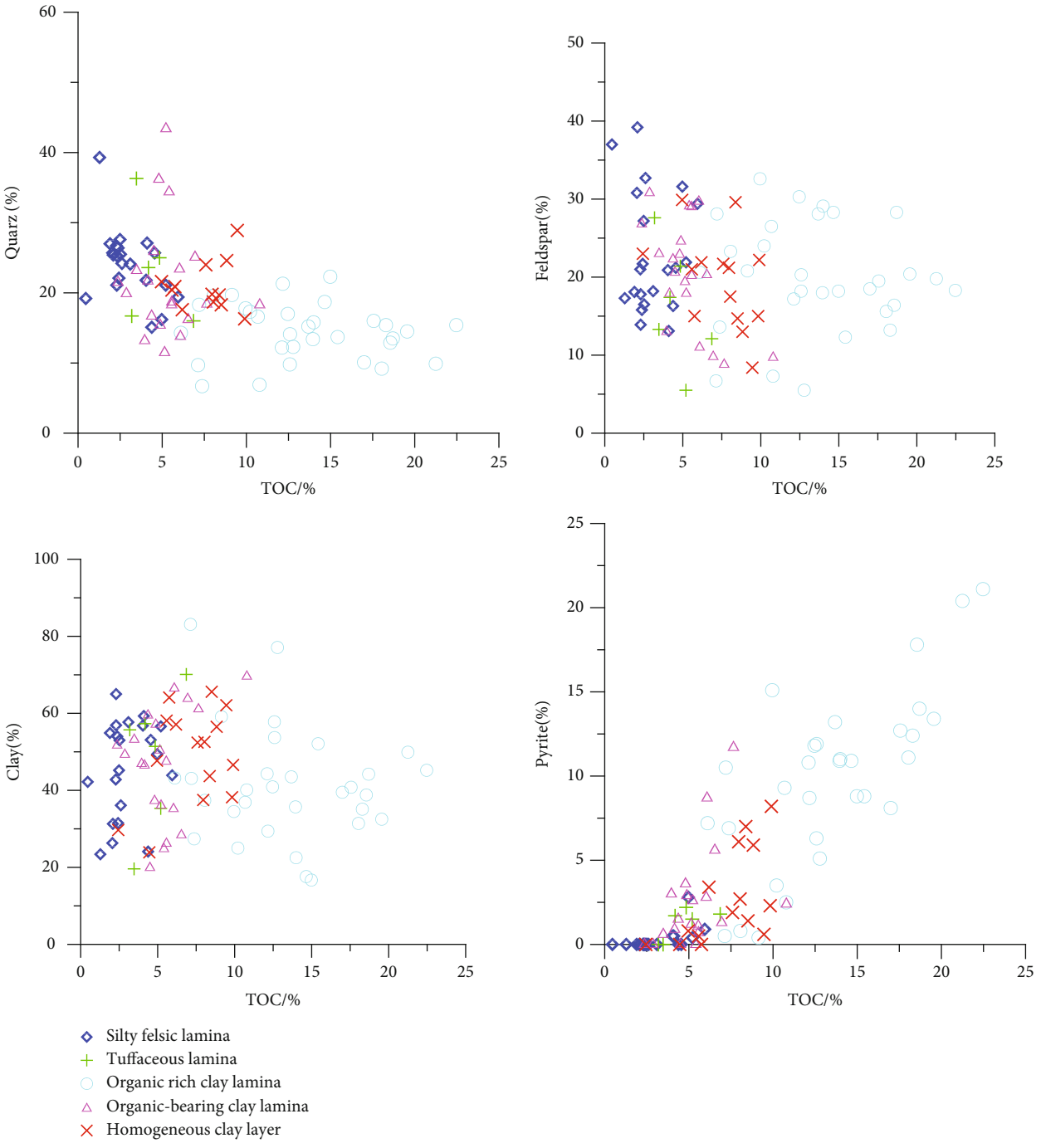

Figure 11: Relationship between TOC and mineral composition of different types of lamina shale of the Chang 7_3 member.

laminae, the TOC of silty felsic laminae is the lowest, so it basically contains no pyrite. The relationship between minerals and organic matter in organic-bearing clay lamina is basically similar to that of silty felsic lamina, except that the content of pyrite increases in the range of 0-10%, which is related to the increase of TOC in this kind of lamina and the enhancement of reducibility of water body. The shale of Qingshankou Formation in the Gulong sag, northern Songliao, also show this law [31], that is, the shale with high TOC (>2-5%) often contains high clay (30-45%) and lower felsic (50-70%) minerals; however, the shale with low TOC (<2) often contains high felsic (65-90%) and lower clay (5-30%) minerals.

The relationship between minerals and organic matter enrichment in organic-rich clay lamina has the largest variation range, which is due to the large variation of TOC in this kind of lamina, which is 6%~24%. However, the TOC of this kind lamina has a significant relationship with quartz and pyrite. When TOC is more than 10%, the content of quartz is obviously less than 20%, while the content of pyrite is more than 10%, which basically represents the strong reduction environment of still water in deep lake area.

However, the content of clay minerals tends to decrease from 50% to 40%, which may be caused by the dilution of organic matter enrichment. The change relationship between minerals and organic matter in homogeneous clay layer is complex, in which the content of feldspar decreases with the increase of TOC, while that of pyrite is the opposite. However, the relationship between the content of quartz and clay minerals and the TOC is not obvious, indicating that the enrichment mechanism of organic matter in this kind of lamina is more complex and there are more influencing factors. For tuffaceous lamina, due to its low organic matter content and small number of laminae, the correlation is not very clear, too.

The development of multiple laminar assemblages at the same depth also has a certain impact on the enrichment of organic matter. Firstly, the tuffaceous lamina developed by volcanic activity dilutes the TOC of the formation due to its low organic matter content or no organic matter. However, tuffaceous matter contains rich nutrients which promote the growth of algae and leads to the rapid enrichment of organic matter in the shale deposited later. Secondly, the activity of silty gravity flow also dilutes the TOC of the formation, damages the anoxic sedimentary and preservation environment, and reduces the TOC of shale deposited nearly the same time.

6. Conclusions

In this study, the laminae of the Chang 7_3 member in well G occur in the form of extreme thin to thin parallel plate-like, and parallel wavy and massive are locally developed. The thickness of a single lamina is between 0.05 and 1.0 mm. According to the shape, thickness, mineral composition, and organic matter content of shale lamina, the lamina types of section Chang 7_3 are divided into 5 types and 7 subtypes.

Shale minerals are mainly composed of clay, feldspar, quartz, and Pyrite, with a small amount of collophanite and carbonate. Clay mainly includes illite and illite/smectite mixed layer. Felsic minerals are mainly quartz, and some of them are developed in the form of siliceous spots and siliceous veins. SEM and probe analysis show that they come from the dissolution and precipitation of SiO_2 in feldspar. Some spherical alga fossils are filled with hydrothermal minerals of different stages, indicating that there was hydrothermal activity in diagenetic stage.

The vertical distribution of shale laminae types in Chang 7_3 member varies greatly. The middle and lower part is mainly rich in ORC and OBC, bearing a small amount of TF, and the upper part is mainly HC and SF. The organic matter in ORC and HC is mainly algae and type I, distributed in dense disseminated or lenticular shape, and the TOC is high, usually greater than 8%. The organic matter in SF and OBC is dominated by type II_1, containing many terrigenous structures, which are sparse dispersed or laminar distribution, and the TOC is usually less than 8%.

Different laminar types deposit different minerals, representing different sedimentary and water environment. The lamina rich in clay, tuffaceous, and pyrite represents large water depth, lack of oxygen at the bottom, less terrigenous input, and good preservation conditions of organic matter, resulting in high TOC and rich shale oil resources. On the contrary, the lamina rich in silt and felsic represents more terrigenous input, turbulent water body, oxidizing environment, and poor preservation conditions of organic matter, leading to low TOC.

Data Availability

Data is not available for confidential reasons.

Conflicts of Interest

The authors declare that they have no conflicts of interest.

Authors' Contributions

Congsheng Bian designed the framework and ideas of the article and wrote the manuscript and polished the language. Wenzhi Zhao put forward research methods, technology, and viewpoint promotion.

Acknowledgments

This study was funded by the National Natural Science Foundation of China (42090020 and 42090025). The PetroChina Changqing Oilfield Company provided the core data. We sincerely appreciate their help.

References

[1] T. X. Jiang, X. B. Bian, H. T. Wang et al., "Volume fracturing of deep shale gas horizontal wells," *Natural Gas Industry*, vol. 37, no. 1, pp. 90–96, 2017.

[2] S. Heng, C. H. Yang, Y. T. Guo, C. Y. Wang, and L. Wang, "Influence of bedding planes on hydraulic fracture propagation in shale formations," *Chinese Journal of Rock Mechanics and Engineering*, vol. 34, no. 2, pp. 4228–4237, 2015.

[3] D. Xu, R. L. Hu, W. Gao, and J. Xia, "Effects of laminated structure on hydraulic fracture propagation in shale," *Petroleum Exploration and Development*, vol. 42, no. 4, pp. 573–579, 2015.

[4] O. R. Lazar, K. M. Bohacs, J. H. S. Macquaker, J. Schieber, and T. M. Demko, "Capturing key attributes of fine-grained sedimentary rocks in outcrops, cores, and thin sections: nomenclature and description guidelines," *Journal of Sedimentary Research*, vol. 85, no. 3, pp. 230–246, 2015.

[5] N. R. O'Brien, "Shale lamination and sedimentary processes," *Geology Socity*, vol. 116, no. 1, pp. 23–36, 1996.

[6] D. Genty and Y. Quinif, "Annually laminated sequences in the internal structure of some Belgian stalagmites; importance for paleoclimatology," *Journal of Sedimentary Research*, vol. 66, no. 1, pp. 275–288, 1996.

[7] C. Liang, Y. Cao, K. Liu, Z. Jiang, J. Wu, and F. Hao, "Diagenetic variation at the lamina scale in lacustrine organic-rich shales: implications for hydrocarbon migration and accumulation," *Geochimica et Cosmochimica Acta*, vol. 229, pp. 112–128, 2018.

[8] Z. Shi, Z. Qiu, D. Dong, B. Lu, P. Liang, and M. Zhang, "Laminae characteristics of gas-bearing shale fine-grained sediment

of the Silurian Longmaxi Formation of Well Wuxi 2 in Sichuan Basin, SW China," *Petroleum Exploration and Development*, vol. 45, no. 2, pp. 358–368, 2018.

[9] K. Xi, K. Li, Y. Cao et al., "Laminae combination and shale oil enrichment patterns of Chang 7 organic-rich shales in the Triassic Yanchang Formation, Ordos Basin, NW China," *Petroleum Exploration and Development*, vol. 47, no. 6, pp. 1342–1353, 2020.

[10] A. Negri, "Possible origin of laminated sediments of the anoxic Bannock Basin (eastern Mediterranean)," *Geo-Marine Letter*, vol. 16, no. 2, pp. 101–107, 1996.

[11] S. F. Leclair and R. W. C. Arnott, "Parallel lamination formed by high-density turbidity currents," *Journal of Sedimentary Research*, vol. 75, no. 1, pp. 1–5, 2005.

[12] D. Walker and J. A. K. Owen, "The characteristics and source of laminated mud at Lake Barrine, Northeast Australia," *Quaternary Science Review*, vol. 18, no. 14, pp. 1597–1624, 1999.

[13] G. M. Barbara and J. Mitchell, "Formation of 30- to 40-micrometer-thick laminations by high-speed marine bacteria in microbial mats," *Applied and Environmental Microbiology*, vol. 62, no. 11, pp. 3985–3990, 1996.

[14] X. Zhang and J. Sha, "Sedimentary laminations in the lacustrine Jianshangou bed of the Yixian formation at Sihetun, western Liaoning, China," *Cretaceous Research*, vol. 36, pp. 96–105, 2012.

[15] D. D. Liu, Z. Li, Z. X. Jiang et al., "Impact of laminae on pore structures of lacustrine shales in the southern Songliao Basin, NE China," *Journal of Asian Earth Sciences*, vol. 182, p. 103935, 2019.

[16] G. L. Hua, S. T. Wu, Z. Qiu, Z. H. Jin, J. L. Xu, and M. D. Guan, "Lamination texture and its effect on reservoir properties: a case study of Longmaxi Shale, Sichuan Basin," *Acta Sedimentologica Sinica*, vol. 39, no. 2, pp. 281–296, 2021.

[17] C. Wang, B. Q. Zhang, Z. G. Shu et al., "Shale lamination and its influence on shale reservoir quality of Wufeng Formation-Longmaxi Formation in Jiaoshiba area," *Earth Science*, vol. 44, no. 3, pp. 972–982, 2019.

[18] R. G. Loucks, R. M. Reed, S. C. Ruppel, and D. M. Jarvie, "Morphology, genesis, and distribution of nanometer-scale pores in siliceous mudstones of the Mississippian Barnett Shale," *Journal of Sedimentary Research*, vol. 79, no. 12, pp. 848–861, 2009.

[19] L. Chen, Z. Jiang, K. Liu et al., "Application of Langmuir and Dubinin-Radushkevich models to estimate methane sorption capacity on two shale samples from the Upper Triassic Chang 7 member in the southeastern Ordos Basin, China," *Energy Exploration Exploitation*, vol. 35, no. 1, pp. 122–144, 2017.

[20] R. Yang, F. Hao, S. He et al., "Experimental investigations on the geometry and connectivity of pore space in organic-rich Wufeng and Longmaxi shales," *Marine and Petroleum Geology*, vol. 84, pp. 225–242, 2017.

[21] W. Yang, R. S. Zuo, Z. X. Jiang et al., "Effect of lithofacies on pore structure and new insights into pore-preserving mechanisms of the over-mature Qiongzhusi marine shales in Lower Cambrian of the southern Sichuan Basin, China," *Marine and Petroleum Geology*, vol. 98, pp. 746–762, 2018.

[22] S. X. Li, X. B. Niu, G. D. Liu et al., "Formation and accumulation mechanism of shale oil in the 7th member of Yanchang Formation, Ordos Basin," *Oil & Gas Geology*, vol. 41, no. 4, pp. 719–729, 2020.

[23] D. M. Jarvie, "Shale resource systems for oil and gas: part 2—shale-oil resource systems," *AAPG Memoir*, vol. 97, pp. 89–119, 2012.

[24] D. M. Jarvie, "Components and processes affecting producibility and commerciality of shale resource systems," *Geologica Acta*, vol. 12, pp. 307–325, 2014.

[25] L. Sun, H. Liu, W. He et al., "An analysis of major scientific problems and research paths of Gulong shale oil in Daqing Oilfield, NE China," *Petroleum Exploration and Development*, vol. 48, no. 3, pp. 527–540, 2021.

[26] Z. Qiu, H. Tao, C. Zou, H. Wang, H. Ji, and S. Zhou, "Lithofacies and organic geochemistry of the Middle Permian Lucaogou Formation in the Jimusar Sag of the Junggar Basin, NW China," *Journal of Petroleum Science and Engineering*, vol. 140, pp. 97–107, 2016.

[27] S. Hu, B. Bai, S. Tao et al., "Heterogeneous geological conditions and differential enrichment of medium and high maturity continental shale oil in China," *Petroleum Exploration and Development*, vol. 49, no. 2, pp. 257–271, 2022.

[28] C. Teichert, "Concepts of facies," *AAPG Bulletin*, vol. 42, no. 11, pp. 2718–2744, 1958.

[29] G. C. Wang and T. R. Carr, "Organic-rich Marcellus Shale lithofacies modeling and distribution pattern analysis in the Appalachian Basin," *AAPG Bulletin*, vol. 97, no. 12, pp. 2173–2205, 2013.

[30] Z. Song, J. Li, X. Li et al., "Coupling relationship between lithofacies and brittleness of the shale oil reservoir: a case study of the Shahejie Formation in the Raoyang Sag," *Geofluids*, vol. 2022, Article ID 2729597, 17 pages, 2022.

[31] B. Liu, H. L. Wang, X. F. Fu et al., "Lithofacies and depositional setting of a highly prospective lacustrine shale oil succession from the Upper Cretaceous Qingshankou Formation in the Gulong sag, northern Songliao Basin, northeast China," *AAPG Bulletin*, vol. 103, no. 2, pp. 405–432, 2019.

[32] C. Y. Liu, J. Q. Wang, D. D. Zhang et al., "Genesis of rich hydrocarbon resources and their occurrence and accumulation characteristics in the Ordos Basin," *Oil & Gas Geology*, vol. 42, no. 5, pp. 1011–1030, 2021.

[33] B. Zhang, Z. Mao, Z. Zhang et al., "Black shale formation environment and its control on shale oil enrichment in Triassic Chang 7 Member, Ordos Basin, NW China," *Petroleum Exploration and Development*, vol. 48, no. 6, pp. 1304–1314, 2021.

[34] G. R. Chalmers, R. M. Bustin, and I. M. Power, "Characterization of gas shale pore systems by porosimetry, pycnometry, surface area, and field emission scanning electron microscopy/transmission electron microscopy image analyses: examples from the Barnett, Woodford, Haynesville, Marcellus, and Doig units," *AAPG Bulletin*, vol. 96, no. 6, pp. 1099–1119, 2012.

[35] E. J. Mathia, L. Bowen, K. M. Thomas, and A. C. Aplin, "Evolution of porosity and pore types in organic-rich, calcareous, Lower Toarcian Posidonia Shale," *Marine and Petroleum Geology*, vol. 75, pp. 117–139, 2016.

[36] M. Wang, R. Ma, J. Li et al., "Occurrence mechanism of lacustrine shale oil in the Paleogene Shahejie Formation of Jiyang Depression, Bohai Bay Basin, China," *Petroleum Exploration and Development*, vol. 46, no. 4, pp. 833–846, 2019.

[37] Y. Y. Chen, S. H. Lin, B. Bai et al., "Effects of petroleum retention and migration within the Triassic Chang 7 Member of the Ordos Basin, China," *International Journal of Coal Geology*, vol. 225, article 103502, 2020.

[38] S. T. Fu, J. L. Yao, S. X. Li, X. P. Zhou, and M. R. Li, "Enrichment characteristics and resource potential of continental shale oil in Mesozoic Yanchang Formation, Ordos Basin," *Petroleum Geology & Experiment*, vol. 42, no. 5, pp. 698–711, 2020.

[39] S. T. Fu, Z. J. Jin, J. H. Fu, S. X. Li, and W. W. Yang, "Transformation of understanding from tight oil to shale oil in the member 7 of Yanchang Formation in Ordos Basin and its significance of exploration and development," *Acta Petrolei Sinica*, vol. 42, no. 5, pp. 561–569, 2021.

[40] S. H. Lin, X. J. Yuan, and Z. Yang, "Comparative study on lacustrine shale and mudstone and its significance: a case from the 7~(th) member of Yanchang Formation in the Ordos Basin," *Oil & Gas Geology*, vol. 38, no. 3, pp. 517–523, 2017.

[41] F. Jinhua, N. Xiaobing, D. Weidong et al., "The geological characteristics and the progress on exploration and development of shale oil in Chang 7 member of Mesozoic Yanchang Formation, Ordos Basin," *China Petroleum Exploration*, vol. 24, no. 5, pp. 601–614, 2019.

[42] G. Liu, Z. Huang, Z. Jiang, J. Chen, C. Chen, and X. Gao, "The characteristic and reservoir significance of lamina in shale from Yanchang Formation of Ordos Basin," *Natural Gas Geoscience*, vol. 26, no. 3, pp. 408–417, 2015.

[43] C. N. Zou, S. Q. Pan, B. Horsfield et al., "Oil retention and intrasource migration in the organic-rich lacustrine Chang 7 shale of the Upper Triassic Yanchang Formation, Ordos Basin, Central China," *AAPG Bulletin*, vol. 10, no. 11, pp. 2627–2663, 2019.

[44] R. L. Ingram, "Terminology for the thickness of stratification and parting units in sedimentary rocks," *GSA Bulletin*, vol. 65, no. 9, pp. 937-938, 1954.

[45] C. V. Campbell, "Lamina, laminaset, bed and bedset," *Sedimentology*, vol. 8, no. 1, pp. 7–26, 1967.

[46] K. K. Huang, S. J. Huang, H. P. Tong, and L. H. Liu, "Thermodynamic calculation of feldspar dissolution and its significance on research of clastic reservoir," *Geological Bulletin of China*, vol. 28, no. 4, pp. 474–482, 2009.

[47] Q. Liu, X. J. Yuan, S. H. Lin, H. Guo, and D. W. Cheng, "Depositional environment and characteristic comparison between lacustrine mudstone and shale: a case study from the Chang 7 member of the Yanchang Formation, Ordos Basin," *Oil & Gas Geology*, vol. 39, no. 3, pp. 531–540, 2018.

[48] F. Liu, X. Zhu, Y. Li et al., "Sedimentary characteristics and facies model of gravity flow deposits of Late Triassic Yanchang Formation in southwestern Ordos Basin, NW China," *Petroleum Exploration and Development*, vol. 42, no. 5, pp. 633–645, 2015.

[49] B. P. Tissot and D. H. Welte, *Petroleum Formation and Occurrence: A New Approach to Oil and Gas Exploration*, Springer, Verlag Berlin Heidelberg, 1978.

[50] M. D. Lewan, M. J. Kotarba, J. B. Curtis, D. Więcław, and P. Kosakowski, "Oil-generation kinetics for organic facies with type-II and -IIS kerogen in the Menilite Shales of the Polish Carpathians," *Geochimica et Cosmochimica Acta*, vol. 70, no. 13, pp. 3351–3368, 2006.

[51] Q. Y. Liu, P. Li, Z. J. Jin et al., "Organic-rich formation and hydrocarbon enrichment of lacustrine shale strata: a case study of Chang 7 member," *Science China Earth Sciences*, vol. 65, no. 1, pp. 118–138, 2022.

[52] A. D. Aubry and P. B. Lauren, "Sediment dispersal and organic carbon preservation in a dynamic mudstone-dominated system, Juana Lopez Member, Mancos Shale," *Sedimentology*, vol. 66, no. 3, pp. 1002–1041, 2019.